Journal of Arid Environments 136 (2017) 19–27

Contents lists available at ScienceDirect

Journal of Arid Environments

journal homepage: www.elsevier.com/locate/jaridenv

# The climate reconstruction potential of *Acacia cambagei* (gidgee) for semi-arid regions of Australia using stable isotopes and elemental abundances

G. Bradd Witt [a, *], Nathan B. English [b], Daniel Balanzategui [c], Quan Hua [d], Patricia Gadd [d], Henk Heijnis [d], Michael I. Bird [e]

[a] The University of Queensland, School of Geography, Planning and Environmental Management, Brisbane, QLD, Australia
[b] Central Queensland University, College of Medical and Applied Sciences, Townsville, QLD, Australia
[c] Section 5.2: Climate Dynamics & Landscape Evolution, Dendrochronology Laboratory, Helmholtz Centre Potsdam, GFZ German Research Centre for Geosciences, Telegrafenberg, D-14473 Potsdam, Germany
[d] Australian Nuclear Science and Technology Organisation, Institute for Environmental Research, Lucas Heights, NSW, Australia
[e] James Cook University, College of Science, Technology and Engineering, Centre for Tropical Environmental and Sustainability Sciences, Townsville, QLD, Australia

ARTICLE INFO

*Article history:*
Received 23 February 2016
Received in revised form
12 August 2016
Accepted 6 October 2016

*Keywords:*
Stable isotopes
ITRAX
Hardwood
Dendrochronology
Climate change
Radiocarbon

ABSTRACT

To provide multi-centennial, annually-resolved records of climate for arid and semi-arid areas of Australia it is necessary to investigate the potential climate signals in tree species in this large region. Using a stable isotope and x-ray fluorescence approach to dendrochronology in *Acacia cambagei*, this study demonstrates short (10 years) proxies of temperature and precipitation are possible. Because rings in *A. cambagei* are difficult to see, precluding traditional dendrochronology, we used elemental abundances of Ca and Sr as an annual chronometer back to 1962. Radiocarbon analysis confirmed that our dating of wood from two trees. We compared $\delta^{13}C$ and $\delta^{18}O$ from the α-cellulose of the dated wood over the most recent 10 years ($n = 10$) to local climate records demonstrating significant relationships between $\delta^{18}O$ and precipitation ($r = -0.85$, $p < 0.002$); mean monthly maximum temperature ($r = 0.69$, $p < 0.03$); and drought indexes (CRU scPDSI 0.5°, $r = -0.89$, $p < 0.001$) for February and March. *Acacia cambagei* may be useful in developing regional networks of climate proxies for drought. Using modern trees, in combination with architectural timbers, it may be possible to construct a multi-century, annually-resolved proxy-record of rainfall and temperature for semi-arid north-eastern Australia.


## 1. Introduction

The intense and prolonged dry and subsequent extreme wet intervals in the first decade of the 21st Century in eastern Australia had catastrophic social, environmental and economic effects. Although ‘drought and flooding rains’ are conspicuous features of Australia's climate, this most recent cycle has received considerable analysis in terms of whether it had any precedents and to what extent the influence of anthropogenic climate change may be superimposed on past climate variability (eg. Kirono et al., 2011; Gergis et al., 2012; Timbal and Fawcett, 2013). For much of eastern Australia, climatic variability over the decade 2002 to 2012 exceeded that of instrumental records (largely limited to the period 1890s to present), leading to great uncertainty among pastoralists, insurers and policy makers about what the climate of the future is likely to hold (CSIRO, 2014).

Significant periods of above and below average rainfall have a strong forcing effect on the vegetation structure and composition (stability) of semi-arid environments, affecting their ability to provide agricultural outputs and to conserve environmental values. Indeed the role of past climate cycles are a key component of debate about the stability of vegetation in these regions (Witt, 2013). There is some emerging and anecdotal evidence that the century between 1760 and 1860 was considerably drier on average than the subsequent century (William Landsborough, cited in The Queenslander, 1877; Lough, 2011). There are also a range of forecasted anthropogenic effects that will have an impact on climate (Kirono et al.,

* Corresponding author.
*E-mail address:* bwitt@uq.edu.au (G.B. Witt).

http://dx.doi.org/10.1016/j.jaridenv.2016.10.002
0140-1963/

2011) and thus the future effects on production and biodiversity are very difficult to predict.

Annually resolved, multi-century climatic reconstructions over several centuries, such as those provided by tree-ring and other chronologies, are required to verify other records and should improve future climate forecasts. Records of past climate change and variability in the semi-arid subtropics of Australia are sparse over the late Holocene and recent centuries (Lough, 2011; Denniston et al., 2013; Haig et al., 2014; Neukom et al., 2014; O'Donnell et al., 2015), yet these unique ecosystems occupy a region impacted by large-scale climate phenomena, including the Sub-Tropical Ridge and El Nino/Southern Oscillation (ENSO), Pacific Decadal Oscillation (PDO) and Interdecadal Pacific Oscillation (IPO) variability (Timbal et al., 2010). Although recent dendrochronology research has been carried out in semi-arid and tropical regions of Australia (Heinrich et al., 2008; Boysen et al., 2014; Baker et al., 2008; Cullen and Grierson, 2009; O'Donnell et al., 2015; O'Donnell et al., 2010), most research has tended to focus on high latitude or other environments with distinct growing seasons (see Heinrich and Allen, 2013). Like many other tropical and subtropical regions of the world, native trees in northern Australia frequently do not meet some of the main assumptions of traditional dendrochronological research methods because radial stem growth may occur more opportunistically, rather than seasonally. However, recent traditional dendrochronological studies and advances in analytical methods, particularly the use of elemental abundance of Calcium (Ca) and Strontium (Sr) measurements using X-ray fluorescence (Martin et al., 2001; Poussart et al., 2006) in concert with well-established bomb radiocarbon methods for accurately validating tree-ring ages (Biondi et al., 2007; Hua et al., 2003; Wood et al., 2010; Pearson et al., 2011) and stable isotopic analysis (particularly $\delta^{13}C$ and $\delta^{18}O$) techniques, have meant that trees in seasonally-dry and tropical and subtropical environments are attracting attention for their climatic and environmental reconstruction potential (Zuidema et al., 2012; Schollaen et al., 2013). What has shown promise for tree species with difficult-to-detect rings is the non-destructive high-resolution (50–200 μm) identification of growth periods through the analysis of relative elemental abundances of Ca and Sr by micro X-ray fluorescence (via ITRAX scanning technology) (Keunecke et al., 2011; Mannes et al., 2007; Heinrich and Allen, 2013; Hietz et al., 2014). Silkin and Ekimova (2012) have demonstrated annual cycles corresponding with increasing abundance of Ca and Sr in particular.

There are already a number of tree species in northern Australia (see Boysen et al., 2014; Baker et al., 2008; Cullen and Grierson, 2007; Pearson et al., 2011; Heinrich and Allen, 2013; O'Donnell et al., 2015) used for dendrochronological research that show promise in terms of their potential for climate reconstruction. *Callitris* spp. have received particular attention in arid and semi-arid regions (see Heinrich and Allen, 2013). While *Agathis* (Boysen et al., 2014) and *Araucaria* (Haines et al., 2015) have been a focus in northern Australian areas receiving higher rainfall. One species that has not received any formal attention is *Acacia cambagei* (gidgee). This highly drought-tolerant tree occurs across much of subtropical semi-arid eastern Australia and is assumed to be long lived as it can reach diameters of 50 cm. This species is resistant to rot and termites, is salt-tolerant, and is both fire-retardant and fire-sensitive (Bui et al., 2014; Nano et al., 2012). Living *A. cambagei* may reflect climate variability spanning possibly a century or so. *Acacia cambagei* was, and continues to be used extensively in the areas where it grows for building construction. Where the date of construction of historical buildings is known, it is likely that these timbers can increase the ability to reconstruct climate back into the early 1800s, and possibly to the time of European colonisation of Australia. This preliminary study explores the potential of *A. cambagei* to serve as a robust climate proxy through the use of micro XRF, bomb radiocarbon dating and stable carbon ($\delta^{13}C$) and oxygen ($\delta^{18}O$) isotope ratios of tree-ring α-cellulose. The resulting $\delta^{18}O$ record is compared to local instrumental climate records to determine its ability to represent past climate in the area. Further research opportunities and dating issues are discussed, however, it does appear that gidgee can assist in climate reconstructions for the large region where it naturally occurs.

## 2. Methods

### 2.1. Study location and climate records

The wood used in this study was collected at Ambathala, a grazing property in south-western Queensland (26°02′24″S: 145°21′22″E) in mid-February 2012 (Fig. 1). Conventional core sampling was not possible due to the density of *A. cambagei* (~1283 kg/m$^3$; Venn and Whittaker, 2003). The growth habit of *A. cambagei* trunks makes it difficult to determine from external observation the internal arrangement of the rings or to identify the 'centre' of the tree (Fig. 2). For these reasons, we felled living trees to examine both the visible rings and their continuity. Many trees in the area have been harvested several times in the past century for construction, fencing, fuel-wood and for thinning to improve pasture production. Cutting was undertaken with the permission of the property owner, and this property has been used for several studies into long-term environmental change in the region in the past decade (Witt et al., 2006, 2009).

Local instrumental precipitation and temperature data from the nearest Bureau of Meteorology recording station at Adavale (approximately 76 km to the west) were compared to stable isotope variation in wood α-cellulose between 2002 and 2011. Ambathala is located in a semi-arid subtropical climate, with the highest rainfall occurring in November through March (40–70 mm/month), also coinciding with the highest temperatures (mean maximum monthly temperature of 21.7 °C). In the winter months, rainfall is generally below 30 mm/month and daily temperatures are still warm (~20 °C). We also used non-detrended 0.5°-gridded (interpolated) temperature and precipitation data set for Australia (CRU TS 3.22) from the Climate Research Unit (University of East Anglia Climatic Research Unit (CRU)) for comparison with the instrumental precipitation and temperature data with the stable isotope records.

### 2.2. Growth ring identification and dating

#### 2.2.1. ITRAX micro x-ray fluorescence and radiography

Our attempts to visually measure rings on eight sanded and polished *A. cambagei* wood discs failed to reliably identify alternating bands earlywood and late wood. Visual ring measurements were hampered by diffuse porous wood, indistinct ring boundaries, vessels in diagonal arrangements, and in some cases wedging, although this could be avoided in most sections. To investigate the possibility that the variability in isotopic ratios and elemental abundances would provide annual markers, we cut 2 cm wide by 5 mm thick radial lengths from two discs of gidgee wood with the least amount of wedging. Based on visual appearance, site location and ringbarking scars we felt these samples might contain the simplest record of isotopic and elemental variability. Elemental abundances were measured from these two trees using the ITRAX core scanner (Croudace et al., 2006) (COX Analytical systems, Sweden) at the Environmental Radioactivity Measurement Centre located at the Australian Nuclear Science and Technology Organisation (ANSTO, Lucas Heights, NSW). Radial lengths were placed on a Perspex block and optical images taken at 200 μm intervals and

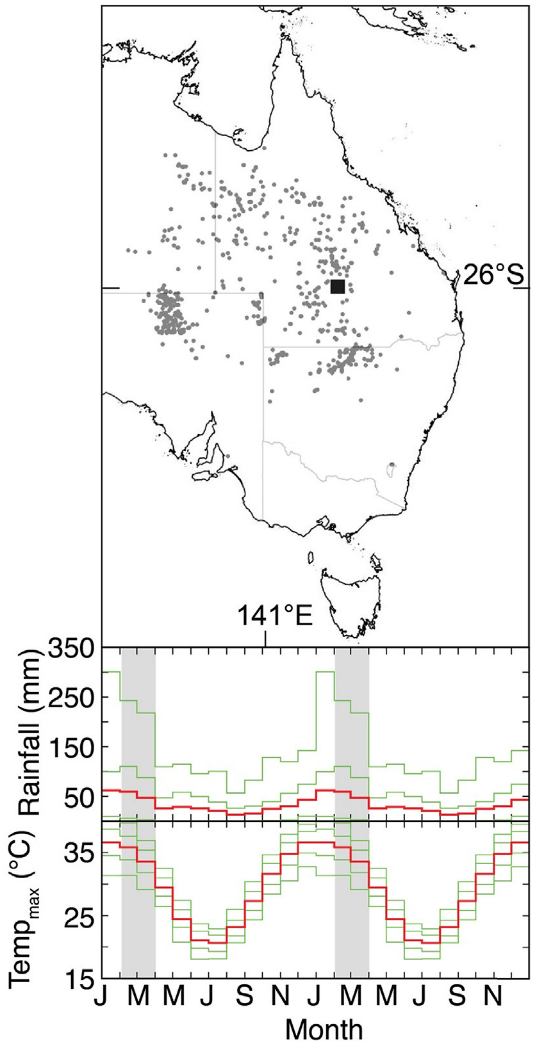


**Fig. 1.** Confirmed occurrences of *Acacia cambagei* (grey dots) and the location of Ambathala (black square), adapted from data available from Australian Living Atlas (http://www.ala.org.au/) (above). Average monthly rainfall and maximum temperature for Adavale (below). The light grey vertical bars indicates the months of February and March which are the focus of the analysis in this study.

stitched together to produce a visual image of the analysed radial length. Radiographs were obtained at 30 kV and 25 mA with an exposure time of 300 ms at 100 μm. Relative elemental abundances were measured every 200 μm using X-ray fluorescence spectroscopy using a Cr-HE tube at 30 kV and 50 mA with 10 s exposures. To more clearly show elemental abundances at the end of the growing season, we did not correct elemental abundance for wood density; and so elemental abundances are shown in counting units.

#### 2.2.2. Radiocarbon dating

From the same radial lengths of wood used for the ITRAX analysis, we used a razor blade to collect raw wood from estimated single "rings" (using presumed-annual variations in elemental abundance in Ca and Sr – see below) of two trees (233 and 238) for radiocarbon measurement to confirm the annual nature of elemental variation in ITRAX data. Two individual rings from each tree were sampled for radiocarbon analysis because bomb $^{14}C$ delivers two possible calendar ages for each measured $^{14}C$ value with one being in the rising and the other in the falling arms of the bomb curve. These collected rings were formed between the late 1950s

**Fig. 2.** Cross-section of *A. cambagei* tree 238 and radial location of ITRAX 238 (black line, line width is ~2 cm). White arrows denote areas showing evidence of ring barking and subsequent recovery and regrowth.

and late 1960s (based on growth ring boundaries identified from Sr and Ca data), the time interval where the differences in atmospheric $^{14}C$ between consecutive years are highest, in order to get the highest accuracy for age determination by the bomb radiocarbon method (Hua, 2009). Radiocarbon samples were pre-treated to α-cellulose (Hua et al., 2004) before being combusted and converted to graphite (Hua et al., 2001) for accelerator mass spectrometry (AMS) $^{14}C$ analysis using the STAR facility at ANSTO (Fink et al., 2004). Radiocarbon values are reported as percent of modern carbon (pMC; Stuiver and Polach, 1977) after normalization to 95% of oxalic acid I (HOx-I) standard and correction for backgrounds (both accelerator and chemistry) and isotope fractionation using measured $\delta^{13}C$. Calendar ages of wood rings from each length were obtained using CaliBomb calibration program (Reimer et al., 2004) with the Southern Hemisphere Zone 1–2 bomb data (Hua et al., 2013) extended back in time by the SHCal13 calibration curve (Hogg et al., 2013).

### 2.3. Stable isotope chronology and development

#### 2.3.1. Stable isotope analysis

For isotope analysis, one radial length from tree 238 (the sample number of one of our two trees, see Table 1) was cut in half in the radial direction (1 cm wide by 5 mm thick) and a 50 μm sample was collected every 200 μm using a rotary microtome starting from the outermost (youngest) section of wood after the bark was removed. We extracted α-cellulose from these samples using the Brendel-method modified for small samples (Brendel et al., 2000). Stable isotope values of carbon ($\delta^{13}C$) and oxygen ($\delta^{18}O$) from α-cellulose ($n = 136$ over 3 days) were measured at the Cairns Analytical Unit (James Cook University, Australia) using a simultaneous measurement approach (Woodley et al., 2011) with a Thermal Conversion/Elemental Analyzer (Thermo Electron Corp, Waltham, MA) attached to a Delta-plus (Thermo Electron Corp, Waltham, MA) continuous flow isotope ratio mass spectrometer. Repeated measurement of our Sigma-Aldrich cellulose working-standards yielded an experimental precision for $\delta^{13}C$ and $\delta^{18}O$ of 0.2‰ and 0.3‰, respectively. While we applied a Suess-correction (Francey et al., 1999; a correction to account for the gradual reduction in atmospheric $\delta^{13}CO_2$ since ~ 1850 CE due to fossil fuel burning) to the $\delta^{13}C$ data, due to all of our samples being consumed in the measurement process we did not apply the pyrolysis adjustment for dual-isotope measurement (Woodley et al., 2011). Due to memory effects, leaving out the 'pyrolysis adjustment' results in underestimating the total variability in the $\delta^{13}C$ record, but does not affect the $\delta^{18}O$

**Table 1**
Ring dates estimated using radiocarbon methods and ring counts estimated from Calcium/Strontium concentrations in cellulose of two *Acacia cambagei* trees from Ambathala, Queensland (pMC is the percent of modern carbon indicting levels of radio carbon above the 1950 level due to atmospheric testing of nuclear weapons).

| Lab ID | Sample ID | $\delta^{13}C$ (‰) | pMC mean | 1σ | Assumed year of growth[a] | Cal. year at 2σ range | Prob. | Year of growth | Errors of ring counts | Interp. |
|---|---|---|---|---|---|---|---|---|---|---|
| OZQ 195 | 2A 238 - 62 | −23.5 | 129.14 | 0.33 | 1962 | 1962.74–1963.33 | 0.09 | 1962 | 0 | **ring count is correct** |
| | | | | | | 1979.10–1982.21 | 0.91 | 1978–1981 | −16 to −19 | |
| OZQ 196 | 2A 238 - 69 | −22.6 | 148.75 | 0.39 | 1969 | 1963.92–1964.26 | 0.04 | 1963 | 6 | |
| | | | | | | 1969.91–1972.87 | 0.95 | 1969–1972 | 0 to −3 | |
| OZQ 197 | 6233 - 62 | −21.8 | 120.00 | 0.31 | 1962 | 1959.92–1963.22 | 0.44 | 1959–1962 | 3 to 0 | **1 false ring or correct ring count** |
| | | | | | | 1985.28–1988.14 | 0.56 | 1984–1987 | −12 to −15 | |
| OZQ 198 | 6233 - 68 | −22.9 | 150.69 | 0.43 | 1968 | 1964.04–1964.40 | 0.05 | 1963 | 5 | |
| | | | | | | 1969.87–1972.21 | 0.95 | 1969–1971 | −1 to −3 | |

[a] Based on Ca and Sr values (see text).

record. Given the short period of time covered in this record (~10 years), the underestimation of $\delta^{13}C$ values is expected to be within the error of the isotope measurement.

### 2.3.2. Age modelling of $\delta^{13}C$ and $\delta^{18}O$ data

In order to compare climate records to our dendrochronological records, tree-ring records must be annually dated. In the case where rings are not visible or are not annual another annual chronometer must be used. Age-modelling (in this case, a combination of manually picking peaks based on elemental abundances and known calibrated $^{14}C$ ages and then interpolating all other points, see below) can then be used to estimate the age of wood at any distance from the pith or bark. Based on the work by Poussart et al. (2006) elemental abundances of Sr and Ca were interpreted as annual variations in growth, irrespective of visible wood structures (Gourlay, 1995; Poussart et al., 2006; Silkin and Ekimova, 2012). Although the mechanisms for Sr and Ca deposition are not fully understood, we have assumed that a key determinant is increasing wood density at the end of the growing season (July to September when it is both cool and dry). Subsequently, if water is available, *A. cambagei* begins to grow again as temperature increases and Ca and Sr abundances decrease with decreasing wood density. We assumed this period to be approximately November in an ‘average year’. However, October through December is traditionally dominated by heterogeneous rainfall from convective storms, which may or may not be adequate to trigger substantial growth. The peak growth in ideal conditions should be in March as water is available and temperatures are cooling down. For these reasons, we hypothesize that the ideal growing period is late summer in average years (February to March). Our data for the end of the record reflects this with very low Sr and Ca values at the time when the tree was cut in mid-February following three of the wettest years in several decades.

We use these assumed seasonal cycles in Ca (“Ca-rings”) to develop an age-model for the stable isotope analyses. The $\delta^{13}C$ and $\delta^{18}O$ analyses were from the same α-cellulose samples that were compared to the Ca and Sr ratios and treated identically for age modelling. Isotope measurements are not evenly distributed among Ca-rings in the radius measured and so we used Matlab (Mathworks, Inc., Natick, MA) to develop and apply an age model that places the isotope analyses in time (years or fractions thereof) rather than space (distance from bark). The age model linearly interpolates the age of distances between each Ca-ring in the series at specified time steps and then interpolates the isotope values over the period of the Ca-ring for those time steps (this method of assigning unevenly spaced data to times series based on $^{14}C$ analysis to check if predicted ages based on elemental variations are correct is described and utilized in English et al., 2010). This yields age-modelled isotope series with roughly the same resolution as the raw isotope series, although the data are now distributed evenly in time. While these data cannot be thought of as seasonally resolved, we can examine the maximum, minimum and mean isotope value of any year and compare those to annual or monthly climate parameters. Age modelling does not require that Ca-rings and stable isotope variation are independent of each other, only that we do not consider climate when developing the age model to avoid “tuning” our data to the climate record we wish to examine.

## 2.4. Statistical analyses

We used simple linear regressions to compare instrumental climate data (Ambathala) with the gridded climate data (CRU) and the age-modelled isotope data. We used KNMI Climate Explorer (Trouet and Van Oldenborgh, 2013) to compare seasonal and transformed Ambathala climate records and age-modelled isotope records with spatially reconstructed climate data from CRU. In KNMI, the correlation coefficients for each 0.5° grid cell reflect simple linear regressions between the data series of interest and the climate time-series in each 0.5° grid cell over the time period selected. In all cases we examined regressions with and without detrending the data sets (simple linear detrending over the length of record examined) and found only small differences in the relationships and significance (Table 2). We use the original data without detrending for this reason. For all statistical analyses reported here (both simple linear regressions and the spatial linear regressions in KNMI), we used KNMI Climate Explorer and $\alpha = 0.05$.

# 3. Results

## 3.1. Ring identification and dating

For all lengths measured, relative elemental abundance of Sr and Ca showed coherent variability throughout the radial lengths

**Table 2**
Simple linear regressions of Adavale monthly climate means and CRU scPDSI with maximum annual $\delta^{18}O$ of cellulose in gidgee. Correlation statistics for both raw and linearly detrended data are shown.

| Variable | Raw | | | Detrended | | |
|---|---|---|---|---|---|---|
| | r | $r^2$ | p | r | $r^2$ | p |
| **$\delta^{18}O_{max}$** | | | | | | |
| Feb–Mar ppt (mm) | −0.85 | 0.72 | 0.002 | −0.82 | 0.67 | 0.004 |
| log(Feb–Mar) ppt | −0.70 | 0.49 | 0.024 | 0.64 | 0.40 | 0.048 |
| Feb–Mar mean $T_{max}$ (°C) | 0.69 | 0.47 | 0.029 | 0.60 | 0.36 | 0.067 |
| CRU scPDSI | −0.89 | 0.78 | 0.001 | −0.87 | 0.76 | 0.001 |
| **log(Feb-Mar) ppt** | | | | | | |
| Feb–Mar mean $T_{max}$ (°C) | −0.67 | 0.44 | <0.0001 | −0.67 | 0.45 | <0.0001 |
| CRU scPDSI | 0.55 | 0.30 | <0.0001 | 0.55 | 0.30 | <0.0001 |

(Fig. 3; simple linear regression, $r = 0.88$, $p < 0.001$, $n = 1089$). Over the 224 mm radial length of tree 238, Sr varied between 278 and 2029 counts, while Ca varied between 7792 and 169,255 counts. We also noted a strong increase in variability at the heart wood/sapwood boundary as found by Poussart et al. (2006), although in our case increased variability appears to carry all the way to the bark. At higher abundances (counts/mm), Ca relative elemental abundances were less noisy than Sr, and so Ca was used to delineate annual years for selecting radiocarbon samples and age modelling. Using the variability in elemental abundances, we estimated that for at least one tree, tree 238, wood from 1940 to the time of collection in early 2012 was present in the 244 mm long radial length (Fig. 3). Radiocarbon analysis of tree-ring material reveals that for two trees (233 and 238), the regular variations in Ca yielded accurate Ca-ring counts back to at least 1962 (Table 1). During very dry seasons or years, we assume that wood formation ceases, and so even though records are presented as continuous they are most likely censored during the driest or hottest seasons and years, leading to lower resolution during those times or even missing years. We reiterate here that the years we have delineated by Ca variability could be wrong and could represent more than one year or less than one year. This “annualization” of an otherwise undated portion of our dated record represents our best, most objective guess of what wood was grown in what year between collection in 2011 and what we believe is 2002.

### 3.2. Stable isotope chronologies

For the outer 28 mm of tree 238, representing 2002 to end of 2011 (Fig. 4), oxygen isotope values ranged from +29.8‰ to +41.2‰ with an average value of +35.6‰, while $\delta^{13}C$ ranged from −22.1‰ to −28.3‰ with an average value of −24.9‰. Over this short length, we observed oscillations of roughly 3‰–6‰ for $\delta^{18}O$ and 2‰–3‰ for $\delta^{13}C$. In the outermost rings from 2009 to the end of 2011 there is a multi-year 7‰ and 3‰ decrease in $\delta^{18}O$ and $\delta^{13}C$, respectively.

The multi-year decrease in stable isotope values coincides with greater precipitation falling in 2010, the end of a decadal drought (Fig. 5). We show preliminary evidence that after the monsoon, increased temperatures and decreased rainfall act in concert to raise soil, xylem and leaf water $\delta^{18}O$ and this is readily recorded as peaks in $\delta^{18}O_{max}$ in α-cellulose of wood grown during that time or shortly thereafter. The peaks and troughs in the $\delta^{18}O$ and $\delta^{13}C$

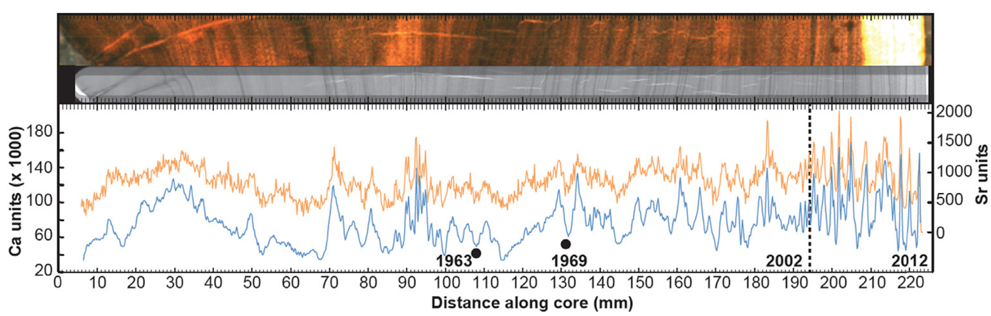


**Fig. 3.** Calcium (blue) and strontium (orange) elemental abundances along core Sample 238. Bark is to the right. Optical and x-ray scans are at top and middle, respectively, and at the same scale as the elemental abundances. Black dots are radiocarbon samples (Table 1) and dashed line and right border are what is shown in Fig. 4. (For interpretation of the references to colour in this figure legend, the reader is referred to the web version of this article.)

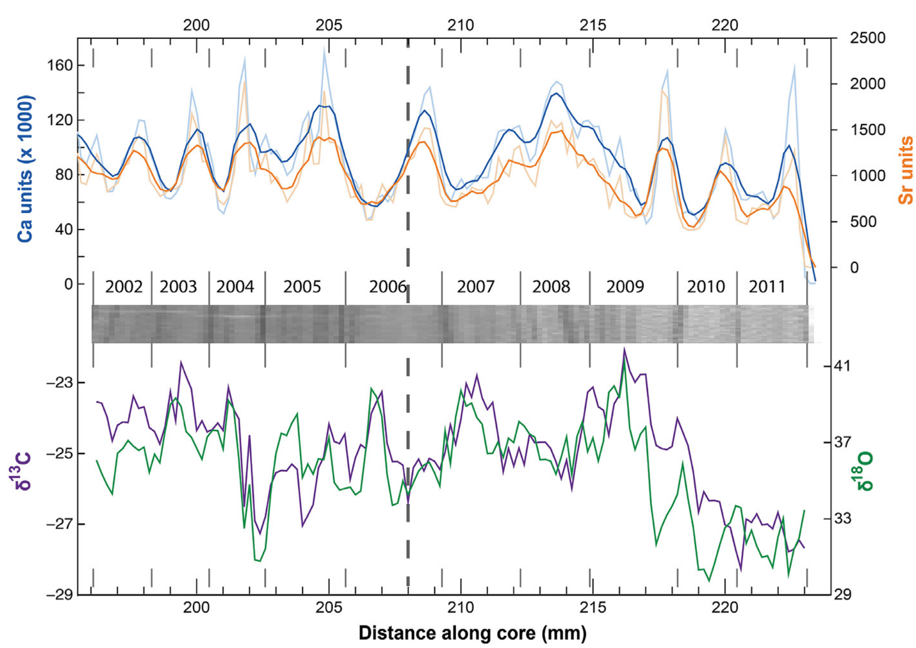


**Fig. 4.** Elemental abundances (Ca blue and Sr Orange with smoothed 5 sample moving average shown as darker line) and Suess corrected $\delta^{13}C$ (purple) and $\delta^{18}O$ (green) for tree 238. Year markers were determined using the ITRAX-derived Ca and Sr elemental abundance in combination with visual identification of rings. The grey dashed line at 208 mm is the heartwood/sapwood boundary as seen in Fig. 3. (For interpretation of the references to colour in this figure legend, the reader is referred to the web version of this article.)

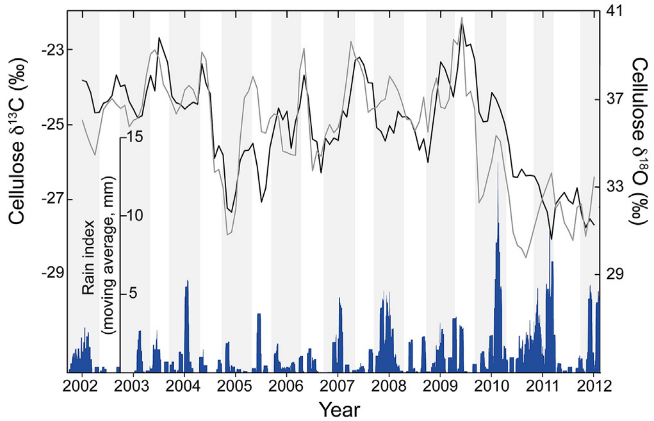


**Fig. 5.** Age-modelled $\delta^{13}C$, $\delta^{18}O$ and rainfall at Adavale. Light grey bars denote hypothesized growing season, blue bars denote 30-day rainfall moving average. There is a sharp decline in $\delta^{13}C$ and $\delta^{18}O$ in 2010 coincident with a significant rainfall increase. While the stable isotope records are presented as continuous, there are most likely growth hiatus present. (For interpretation of the references to colour in this figure legend, the reader is referred to the web version of this article.)

record correspond to what we believe are the growing seasons of *A. cambagei* at this site and are consistent with calendar year boundaries picked using Ca elemental abundances. From year-to-year, including late 2011, lower $\delta^{18}O$ (troughs) occur in wet, monsoon conditions as water in shallow soil is recharged and vapour pressure deficit (VPD) declines, reducing evaporative demand on leaves. These seasonal variations are also in line with the hypothesis that $\delta^{18}O$ reflects drought severity, with higher $\delta^{18}O$ (peaks) coinciding with post-monsoon conditions with higher temperature, higher VPD and decreased rainfall and soil water availability. Over a whole year, increasingly severe drought as measured by Self-calibrating Palmer Drought Severity Index (scPDSI) (Wells et al., 2004) corresponds to higher maximum $\delta^{18}O$ values. An exception to this is the $\delta^{18}O_{max}$ in α-cellulose for driest year on record at this site, 2005. We speculate that the extreme drought conditions caused the plant to either rely to a greater extent on deeper ground-water with lower $\delta^{18}O$ values or that growth ceased before $\delta^{18}O$ reached extremely high values. Because we do not know the reason for this outlier, we have left it in our regressions (Table 2) but examined its effect on our models if removed (Fig. 6c and d). Although not as clear as in the $\delta^{18}O$ data, in water limited environments increasing $\delta^{13}C$ values should coincide with the hot, dry portion of the year as stomata close to conserve water and discrimination decreases (Scheidegger et al., 2000). Over the ten years of record we observed no significant correlations between $\delta^{13}C$ and local climate.

There were, however, significant and strong relationships between the annualized $\delta^{18}O_{max}$ (the maximum $\delta^{18}O$ value occurring within an annual ring) and local climate (Fig. 6, Table 2). As we hypothesized, $\delta^{18}O_{max}$ was negatively related to total precipitation in February and March (the most likely growing season for *A. cambagei*) at Adavale (Fig. 6B; $r = -0.85$; $p = 0.002$, $n = 10$). Likewise, $\delta^{18}O_{max}$ was positively related to mean maximum temperature in February and March at Adavale (Fig. 6C; $r = 0.69$; $p < 0.03$, $n = 10$). At Adavale, February and March temperature and

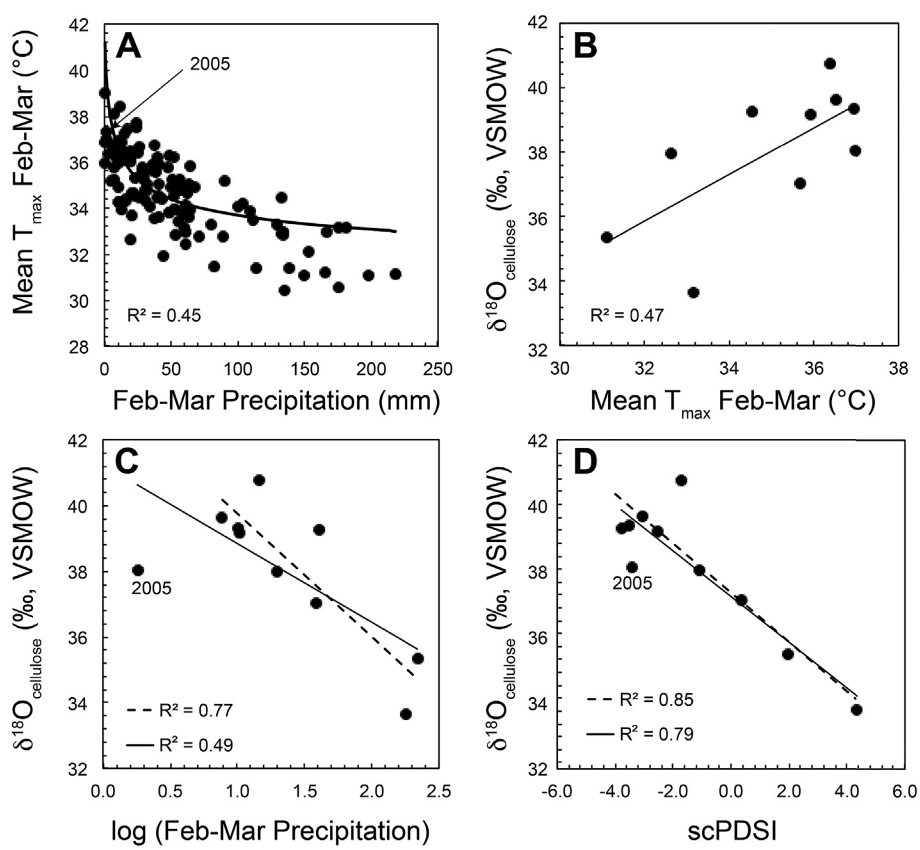


**Fig. 6.** Simple linear regressions and Pearson-correlation coefficients of (A) mean maximum temperature with total precipitation (1901–2011) at Adavale; annual maximum $\delta^{18}O$ in the α-cellulose of *Acacia cambagei* (2002–2011) with (B) mean maximum temperature; (C) the log of precipitation (the linear regression is against the log values, not shown here); and (D) self-calibrated Palmer Drought Severity Index (+ = wetter). Dashed lines in bottom panels are linear regressions without Feb–Mar 2005, the driest February–March (2 mm total precipitation) over the isotope record (see text in section 3.2).

precipitation are negatively correlated (Fig. 6A; $r = -0.67$; $p < 0.0001$, $n = 111$). The relationship of $\delta^{18}O_{max}$ with scPDSI remains significant when tested using a non-parametric statistic (Spearman's rank order correlation, $p(8) = -0.66$, $p = 0.038$, $\alpha = 0.05$ on non-detrended data), although the relationship of $\delta^{18}O_{max}$ with mean maximum temperature in February and March and total precipitation in February and March is only significant ($p < 0.05$) if a one-tailed test is considered. The strong relationship between rainfall and temperature at Adavale and regional rainfall, temperature and scPDSI (Fig. 7A,C,E) and the strong relationship between $\delta^{18}O_{max}$ of *A. cambagei* cellulose and Adavale precipitation and temperature (Fig. 7B,D,F) leads us to very cautiously suggest that variability in $\delta^{18}O_{max}$ of *A. cambagei* cellulose may reflect drought intensity in large portions of southwestern Queensland, northern New South Wales and eastern South Australia and Northern Territory. This suggestion is in line with other work on isotopes in tropical and sub-tropical trees that find significant associations between $\delta^{18}O$ and local, regional and global climate phenomena (Boysen et al., 2014; Poussart et al., 2004).

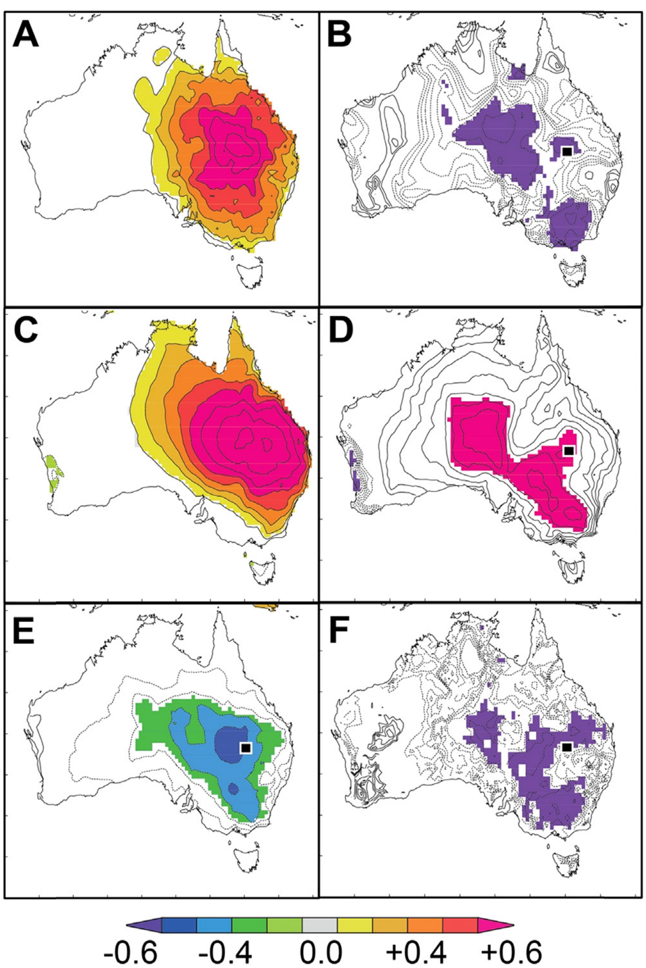


**Fig. 7.** Spatial pearson-correlation coefficients (colour bars; only coloured grid cells have correlations significant at $p < 0.05$) for February and March of (A) mean February–March monthly precipitation at Adavale (instrumental) with Australian mean February–March precipitation (1901–2011, CRU gridded); (B) Australian February–March precipitation total (2002–2011, CRU gridded) with maximum $\delta^{18}O$ in the $\alpha$-cellulose of *A. cambagei*; (C) mean February–March maximum temperature at Adavale (instrumental) with Australian monthly mean maximum temperatures (1901–2011, CRU gridded); (D) mean Australian February–March maximum temperatures (2002–2011, CRU gridded) with maximum $\delta^{18}O$ in the $\alpha$-cellulose of *A. cambagei*; (E) log of February–March monthly precipitation at Adavale (instrumental) with Australian mean February–March maximum temperatures (1901–2011, gridded); and (F) self-calibrating PDSI (CRU, gridded) with maximum $\delta^{18}O$ in the $\alpha$-cellulose of *A. cambagei*. (For interpretation of the references to colour in this figure legend, the reader is referred to the web version of this article.)

## 4. Discussion

This study supports recent work that demonstrates the ability for micro XRF to assist in the dating of tree rings in semi-arid and subtropical environments where traditional dendrochronological methods have been rarely employed (Zuidema et al., 2012), and that drought appears to have a strong influence on wood cellulose of *Acacia cambagei*. For two trees, we were able to accurately date material in the rings back to the 1960s (ie. >50 years) from today using Ca abundances in wood with indistinct rings. Although we have not been able to do so here, once elemental abundance oscillations have been shown to be annual, the use of $\delta^{18}O$ provides a proxy for rainfall, temperature, and drought particularly during the late-summer monsoon season (February–March). Records such as this may be useful in extending the spatial coverage of the Asian Monsoon drought index (Cook et al., 2010) or filling in the Australia-New Zealand Drought Atlas (Palmer et al., 2015). The variability in our stable isotope records is consistent with annual and seasonal changes in temperature and rainfall at Ambathala. Specifically, $\delta^{18}O_{max}$ of $\alpha$-cellulose are correlated with temperature and precipitation (February and March).

Although it would be expected that $\delta^{13}C$ in $\alpha$-cellulose should also be indicative of water stress and temperature, our $\delta^{13}C$ results are inconclusive and align with work on *Callitris columellaris* by Cullen and Grierson (2007). This does not preclude $\delta^{13}C$ from future climate reconstruction work as it has been demonstrated in *Acacia* spp. of semi-arid Ethiopia to correlate very well with precipitation, but not temperature, particularly for deciduous taxa, (Gebrekirstos et al., 2009). This highlights the need for a more detailed understanding of assimilation, conductance and water use efficiency, climate and stable isotope in wood cellulose $\delta^{13}C$. However, the simple assumption that there is a relationship between $\delta^{13}C$ in wood cellulose, rainfall and temperature (and thus water stress) does not appear to be the case here.

The use of micro XRF and $\delta^{18}O$ in $\alpha$-cellulose, in concert with radiocarbon dating, shows promise for using the wide-spread tree, *A. cambagei*, for dendrochronological and climate research. The *A. cambagei* from southwest Queensland used in this study suggest that archives of rainfall variability over much of inland Australia extending through southwest Queensland into western NSW and then into south-eastern Australia may be derived from this species using dendro-chemistry. The preliminary decade-long record presented here spans some of the driest and wettest years since records for the region began, and this variability is captured in the $\delta^{18}O$ tree rings of *A. cambagei*. The Ambathala shearing-shed was built at the turn of the century and is set upon over 100 well-preserved *A. cambagei* stumps. Building of similar stature and age are located across the geographic range of this species and date back to the late 1800s. Based on this research it may be that, when both standing and architectural wood are dated and analysed, to reconstruct a temperature- and rainfall-proxy record for inland parts of Australia dating back at least 100 years before the beginning of instrumental records.

## Acknowledgements

This work was partially funded by AINSE (ALNGRA12098), The School of Geography Planning and Environmental Management (The University of Queensland), and an Australian Research Council Discovery Early Career Researcher Award (DE130100295). The work would not have been possible without the support and access to

Ambathala granted by the property owners. We're also grateful to Drs. Jen Whan and Chris Wurster for their assistance in the Cairns Analytical Laboratory.

## References


Baker, P., Palmer, J., D'Arrigo, R., 2008. The dendrochronology of *Callitris intratropica* in northern Australia: annual ring structure, chronology development and climate correlations. Aust. J. Bot. 56, 311–320.

Biondi, F., Strachan, S., Mensing, S., Piovesan, G., 2007. Radiocarbon analysis confirms the annual nature of sagebrush growth rings. Radiocarbon 49, 1231–1240.

Boysen, B., Evans, M., Baker, P., 2014. $\delta^{18}O$ in the tropical conifer Agathis robusta records ENSO-related precipitation variations. PLoS One 9 (7), e102336. http://dx.doi.org/10.1371/journal.pone.0102336.

Brendel, O., Iannetta, P., Stewart, D., 2000. A rapid and simple method to isolate pure alpha-cellulose. Phytochem. Anal. 11, 7–10.

Bui, E.N., González-Orozco, C.E., Miller, J.T., 2014. *Acacia*, climate, and geochemistry in Australia. Plant Soil 381, 161–175.

Cook, E.R., Anchukaitis, K.J., Buckley, Brendan M., D'Arrigo, R.D., Jacoby, G.C., Wright, William E., 2010. Asian monsoon failure and megadrought during the last millennium. Science 328, 486–489.

Croudace, I.W., Rindby, A., Rothwell, R.G., 2006. ITRAX: description and evaluation of a new multi-function X-ray core scanner. Special Publ. Geol. Soc. Lond. 267, 51.

University of East Anglia Climatic Research Unit (CRU) CRU TS3.21: Climatic Research Unit (CRU) Time-Series (TS) Version 3.21 of High Resolution Gridded Data of Month-by-month Variation in Climate (Jan. 1901-Dec. 2012), [Internet]. Jones, P., Harris, I. (Eds.).

CSIRO, Australian Bureau of Meteorology, 2014. State of the Climate, 16 p.

Cullen, L.E., Grierson, P.F., 2007. A stable oxygen, but not carbon, isotope chronology of *Callitris columellaris* reflects recent climate change in north-western Australia. Clim. Change 85, 213–229.

Cullen, L.E., Grierson, P.F., 2009. Multi-decadal scale variability in autumn-winter rainfall in south-western Australia since 1655 AD as reconstructed from tree rings of *Callitris columellaris*. Clim. Dyn. 33, 433–444. http://dx.doi.org/10.1007/s00382-008-0457-8.

Denniston, R.F., Wyrwoll, K.-H., Polyak, V.J., Brownd, J.R., Asmeromc, Y., Wanamaker Jr., A.D., LaPointe, Z., Ellerbroek, R., Barthelmes, M., Cleary, D., Cugley, J., Woods, D., Humphreys, W.F., 2013. A Stalagmite record of Holocene Indonesian-Australian summer monsoon variability from the Australian tropics. Quat. Sci. Rev. 78, 155–168.

English, N.B., Dettman, D.L., Williams, D.G., 2010. A 26-year stable isotope record of humidity and El Nino-enhanced precipitation in the spines of saguaro cactus, Carnegiea gigantea. Paleogeogr. Paleoclimatology, Paleoecol. 293, 108–119.

Fink, D., Hotchkis, M., Hua, Q., Jacobsen, G., Smith, A.M., Zoppi, U., Child, D., Mifsud, C., van der Gaast, H., Williams, A., Williams, M., 2004. The ANTARES AMS facility at ANSTO. Nucl. Instrum. Methods Phys. Res. Sect. B 223–224, 109–115.

Francey, R.J., Allison, C.E., Etheridge, D.M., Trudinger, C.M., Enting, I.G., Leuenberger, M., Langenfelds, R.L., Michel, E., Steele, L.P., 1999. A 1000-year high precision record of $\delta^{13}C$ in atmospheric $CO_2$. Tellus 51B, 170–193.

Gebrekirstos, A., Worbes, M., Teketay, D., Fetene, M., Mitlöhner, R., 2009. Stable carbon isotope ratios in tree rings of co-occurring species from semi-arid tropics in Africa: patterns and climatic signals. Glob. Planet. Change 66, 253–260.

Gergis, J., Gallant, A.J.E., Braganza, K., Karoly, D.J., Allen, K., Cullen, L., D'Arrigo, R., Godwin, I., Grierson, P., McGregor, S., 2012. On the long-term context of the 1997–2009 'Big Dry' in South-Eastern Australia: insights from a 206-year multi-proxy rainfall reconstruction. Clim. Change 111, 923–944.

Gourlay, I., 1995. Growth ring characteristics of some African *Acacia* species. J. Trop. Ecol. 11, 121–140.

Haig, J., Nott, J., Reichart, G.-J., 2014. Australian tropical cyclone activity lower than at anytime over the past 550–1,500 years. Nature 505, 667–671.

Haines, H., English, N., Olley, J., Hua, Q., Heijnis, H., Palmer, J., 2015. Identifying Flood and Drought Events Using a 500-year Reconstruction of Rainfall in the Australian Subtropics as Determined from Hoop Pine (*Araucaria cunninghamii*) Tree Rings. The 19th INQUA Congress, 27 Jul – 2 Aug 2015, Nagoya, Japan.

Heinrich, I., Allen, K., 2013. Current issues and recent advances in Australian dendrochronology: where to next? Geogr. Res. 51, 180–191.

Heinrich, I., Weidner, K., Helle, G., Vos, H., Banks, J.C., 2008. Hydroclimatic variation in Far North Queensland since 1860 inferred from tree rings. Palaeogeogr. Palaeoclimatol. Palaeoecol. 270, 116–127.

Hietz, P., Horsky, M., Prohaska, T., Lang, I., Grabner, M., 2014. High-resolution densitometry and elemental analysis of tropical wood. Trees 29, 487–497.

Hogg, A.G., Hua, Q., Blackwell, P.G., Niu, M., Buck, C.E., Guilderson, T.P., Heaton, T.J., Jonathan G Palmer, J.G., Reimer, P.J., Reimer, R.W., Turney, C.S.M., Zimmerman, S.R.H., 2013. SHCAL13 southern Hemisphere calibration, 0–50,000 Years cal Bp. Radiocarbon 55, 1889–1903.

Hua, Q., 2009. Radiocarbon: a chronological tool for the recent past. Quat. Geochronol. 4, 378–390.

Hua, Q., Jacobsen, G.E., Zoppi, U., Lawson, E.M., Williams, A.A., Smith, A.M., McGann, M.J., 2001. Progress in radiocarbon target preparation at the ANTARES AMS Centre. Radiocarbon 43, 275–282.

Hua, Q., Barbetti, M., Zoppi, U., Chapman, D.M., Thomson, B., 2003. Bomb radiocarbon in tree-rings from northern New South Wales, Australia: implications for dendrochronology, atmospheric transport and air-sea exchange of $CO_2$. Radiocarbon 45, 431–447.

Hua, Q., Barbetti, M., Zoppi, U., Fink, D., Watanasak, M., Jacobsen, G.E., 2004. Radiocarbon in tropical tree rings during the little ice age. Nucl. Instrum. Methods Phys. Res. B 223–224, 489–494.

Hua, Q., Barbetti, M., Rakowski, A.Z., 2013. Atmospheric radiocarbon for the period 1950-2010. Radiocarbon 55, 2059–2072.

Keunecke, D., Novosseletz, K., Lanvermann, C., Mannes, D., Niemz, P., 2011. Combining X-ray imaging and digital image correlation to analyse strain in wood: potential and difficulties. Wood Res. 55, 49–59.

Kirono, D.G.C., Kent, D.M., Hennessy, K.J., Mpelasoka, F., 2011. Characteristics of Australian droughts under enhanced greenhouse conditions: results from 14 global climate models. J. Arid Environ. 75, 566–575.

Lough, J.M., 2011. Great Barrier Reef coral luminescence reveals rainfall variability over northeastern Australia since the 17th century. Paleoceanography 26, PA2201. http://dx.doi.org/10.1029/2010PA002050.

Mannes, D., Lehmann, E., Cherubini, P., Niemz, P., 2007. Neutron imaging versus standard X-ray densitometry as method to measure tree-ring wood density. Trees 21, 605–612, 16.

Martin, R., Sham, T., Won, G.W., Jones, K., Feng, H., 2001. Synchrotron X-ray fluorescence and secondary ion mass spectrometry in tree ring microanalysis: applications to dendroanalysis. X Ray Spectrom. 30, 338–341.

Nano, C.E.M., Bowland, A.E., Nano, T.J., Raghub, S., Paveya, C.R., 2012. Demographic hurdles to persistence in *Acacia peuce* (F. Muell.): effects of resources, fire and browsing on a threatened keystone tree species from arid Australia. J. Arid Environ. 80, 17–26.

Neukom, R., Gergis, J., Karoly, D.J., Wanner, H., Curran, M., Elbert, J., González-Rouco, F., Linsley, B.K., Moy, A.D., Mundo, I., Raible, C.C., Steig, E.J., van Ommen, T., Vance, T., Villalba, R., Zinke, J., Frank, D., 2014. Inter-hemispheric temperature variability over the past millennium. Nat. Clim. Change 4, 362–367. http://dx.doi.org/10.1038/NCLIMATE2174.

O'Donnell, A.J., Cook, E.R., Palmer, J.G., Turney, C.S.M., Page, G.F.M., Grierson, P.F., 2015. Tree rings show recent high summer-autumn precipitation in Northwest Australia is unprecedented within the last two centuries. PLoS One 10 (6), e0128533. http://dx.doi.org/10.1371/journal.pone.0128533.

O'Donnell, A.J., Cullen, L.E., McCaw, W.L., Boer, M.M., Grierson, P.F., 2010. Dendroecological potential of *Callitris preissii* for dating historical fires in semi-arid shrublands of southern Western Australia. Dendrochronologia 28, 37–48.

Palmer, J.G., Cook, E.R., Turney, C.S.M., Allen, K., Fenwick, P., Cook, B.I., O'Donnell, A., Lough, J., Grierson, P., Baker, P., 2015. 2015. Drought variability in the eastern Australia and New Zealand summer drought atlas (ANZDA, CE 1500–2012) modulated by the Interdecadal Pacific Oscillation. Environ. Res. Lett. 10, 124002.

Pearson, S., Hua, Q., Allen, K., Bowman, D.M.J.S., 2011. Validating putatively cross-dated *Callitris* tree-ring chronologies using bomb-pulse radiocarbon analysis. Aust. J. Bot. 59, 7–17.

Poussart, P.M., Myneni, S.C.B., Lanzirotti, A., 2006. Tropical dendrochemistry: a novel approach to estimate age and growth from ringless trees. Geophys. Res. Lett. 33, L17711. http://dx.doi.org/10.1029/2006GL026929.

Reimer, P.J., Brown, T.A., Reimer, R.W., 2004. Discussion: reporting and calibration of post-bomb $^{14}C$ data. Radiocarbon 46, 1299–1304.

Scheidegger, Y., Saurer, M., Bahn, M., Siegwolf, R., 2000. Linking stable oxygen and carbon isotopes with stomatal conductance and photosynthetic capacity: a conceptual model. Oecologia 125, 350–357.

Schollaen, K., Heinrich, I., Neuwirth, B., Krusic, P.J., D'Arrigo, R.D., Karyanto, O., Helle, G., 2013. Multiple tree-ring chronologies (ring width, δ13C and δ18O) reveal dry and rainy season signals of rainfall in Indonesia. Quat. Sci. Rev. 73, 170–181.

Silkin, P.P., Ekimova, N.V., 2012. Relationship of strontium and calcium concentrations with the parameters of cell structure in Siberian spruce and fir tree-rings. Dendrochronologia 30, 189–194.

Stuiver, M., Polach, H.A., 1977. Reporting of 14C data. Radiocarbon 19, 353–363.

The Queenslander, 1877. Australia becoming a Wetter Country, 13th April, 1877 page 12. available online: http://trove.nla.gov.au.

Timbal, B., Fawcett, R., 2013. A historical perspective on Southeastern Australian rainfall since 1865 using the instrumental record. J. Clim. 26, 1112–1129.

Timbal, B., Arblaster, J., Braganza, K., Fernandez, E., Hendon, H., Murphy, B., Raupach, M., Rakich, C., Smith, I.K.W., Wheeler, M., 2010. Understanding the Anthropogenic Nature of the Observed Rainfall Decline across South Eastern Australia. Centre for Australian Weather and Climate Research (CAWCR), p. 202. Technical Report No. 026.

Trouet, V., Van Oldenborgh, G.J., 2013. KNMI Climate Explorer: a web-based research tool for high-resolution paleoclimatology. Tree-Ring Res. 69, 3–13.

Venn, T.J., Whittaker, K., 2003. Potential specialty timber markets for hardwoods of western Queensland, Australia. Small-scale For. Econ. Manag. Policy 2, 377–395.

Wells, N., Goddard, S., Hayes, M.J., 2004. A self-calibrating palmer drought severity index. J. Clim. 17, 2335–2351.

Witt, G.B., 2013. Vegetation changes through the eyes of the locals: the 'artificial wilderness' in the mulga country of south-west Queensland. Rangel. J. 35, 299–314.

Witt, G.B., Luly, J., Fairfax, R.J., 2006. How the west was once: vegetation change in south-west Queensland from 1930 to 1995. J. Biogeogr. 33, 1585–1596.

Witt, G.B., Harrington, R.A., Page, M.J., 2009. Is vegetation thickening occurring in Queenslands mulga lands? A 50-year aerial photographic analysis. Aust. J. Bot.

57, 572–582.
Wood, S.W., Hua, Q., Allen, K.J., Bowman, D.M.J.S., 2010. Age and growth of a fire prone Tasmanian temperate old-growth forest stand dominated by Eucalyptus regnans, the world's tallest angiosperm. For. Ecol. Manag. 260, 438–447.
Woodley, E.J., Loader, N.J., McCarroll, D., Young, G.H.F., Robertson, I., Heaton, T.H.E., Gagen, M.H., Warham, J.O., 2011. High-temperature pyrolysis/gas chromatography/isotope ratio mass spectrometry: simultaneous measurement of the stable isotopes of oxygen and carbon in cellulose. Rapid Commun. Mass Spectrom. 26, 109–114.
Zuidema, P.A., Brienen, R.J.W., Schoengart, J., 2012. Tropical forest warming: looking backwards for more insights. Trends Ecol. Evol. 27, 193–194.